

Distribution Agreement

In presenting this thesis as a partial fulfillment of the requirements for a degree from Emory University, I hereby grant to Emory University and its agents the non-exclusive license to archive, make accessible, and display my thesis in whole or in part in all forms of media, now or hereafter now, including display on the World Wide Web. I understand that I may select some access restrictions as part of the online submission of this thesis. I retain all ownership rights to the copyright of the thesis. I also retain the right to use in future works (such as articles or books) all or part of this thesis.

Maddie Hasson

April 10, 2024

Guiding Cell Perception of its Microenvironment for Enhanced Microfracture Repair

by

Maddie Hasson

Dr. Jay Patel
Adviser

Department of Anthropology

Dr. Jay Patel
Adviser

Dr. Craig Hadley
Committee Member

Dr. Edward Nam
Committee Member

2024

Guiding Cell Perception of its Microenvironment for Enhanced Microfracture Repair

By

Maddie Hasson

Dr. Jay Patel

Adviser

An abstract of
a thesis submitted to the Faculty of Emory College of Arts and Sciences
of Emory University in partial fulfillment
of the requirements of the degree of
Bachelor of Science with Honors

Department of Anthropology

2024

Abstract

Guiding Cell Perception of its Microenvironment for Enhanced Microfracture Repair

By Maddie Hasson

Introduction: Cartilage injuries impose significant societal and economic burdens, but limited treatment options are available. Microfracture is the current gold standard for cartilage injury but often leads to suboptimal outcomes, necessitating better chondrogenic therapies. The microfracture repair environment may be thoroughly explored by developing a fibrin-based gel model. Leveraging inhibition of the Rho/ROCK pathway, a signaling pathway involved in cell contractility, along with Transforming Growth Factor Beta 3 (TGF- β 3), this research aims to enhance cartilage regeneration post-microfracture by elucidating cellular behavior and matrix organization within the clot environment.

Materials/Methods: Fibrin gels were synthesized and characterized by evaluating bulk mechanics, contraction, and visualizing fiber formation using scanning electron microscopy (SEM). Cell behavior in response to Rho/ROCK inhibition (Fasudil) and TGF- β 3 was evaluated by quantifying cell mechanics and staining for SMAD 2/3 and stress fibers after three days. Long-term macroscale gel activity after Fasudil and TGF- β 3 treatment was assessed by tracking contraction, evaluating proteoglycan deposition, and quantifying relative gene expression after four weeks in culture.

Results: After four weeks, low-thrombin fibrin gels contracted significantly compared to high-thrombin gels. Nanoindentation revealed reduced effective Young's modulus in Rho/ROCK-inhibited cells, which was maintained after addition of TGF- β 3. Stress fiber formation in Rho/ROCK-inhibited cells was attenuated compared to controls. We observed a stepwise trend in SMAD 2/3 nuclear intensity in cells treated with Fasudil, TGF- β 3, and Fasudil with TGF- β 3. Fasudil mitigated gel contraction compared to controls, and a 9-fold increase in type-II collagen expression was observed in gels cultured with Fasudil alone, whereas a ~200-fold increase was observed in gels cultured with Fasudil and TGF- β 3.

Discussion: Higher thrombin concentrations and treatment with Fasudil modify the extracellular microenvironment and cellular machinery in a way that prevents macroscale contraction. Fasudil and TGF- β 3 treatment significantly enhances type-II collagen deposition over four weeks, while simultaneously reducing contraction. This combined effect suggests that Fasudil helps maintain defect fill while simultaneously promoting cartilage regeneration.

Clinical Relevance: Understanding the roles of the extracellular matrix organization and cell contractility in the early microfracture environment may provide insight into material-based or pharmacological treatments for improving the outcomes of microfracture.

Guiding Cell Perception of its Microenvironment for Enhanced Microfracture Repair

By

Maddie Hasson

Dr. Jay Patel

Adviser

A thesis submitted to the Faculty of Emory College of Arts and Sciences
of Emory University in partial fulfillment
of the requirements of the degree of
Bachelor of Science with Honors

Department of Anthropology

2024

Acknowledgements

I extend my deepest gratitude to Dr. Jay Patel for providing me with the amazing opportunity to work in his lab over the past four years. His mentorship, guidance, and unwavering support have been instrumental in shaping my academic and personal growth. Dr. Patel's dedication to fostering a nurturing research environment has been and continues to be a constant source of inspiration, and his expertise has greatly enriched my understanding of scientific inquiry.

I would also like to express my appreciation to my exceptional lab mates, Hanna Solomon, Adi Pucha, Nick Huffman, and Lorenzo Fernandes. Their camaraderie, encouragement, and collaborative spirit have made my research journey immensely rewarding. Together, we have navigated through challenges, celebrated successes, and collectively contributed to advancing our understanding of the fibrin clot and the microfracture environment.

Furthermore, I am grateful to Dr. Edward Nam and Dr. Craig Hadley for their unwavering support and trust in my abilities. Their mentorship and encouragement have played a pivotal role in shaping my academic endeavors and instilling confidence in my capabilities. I am deeply thankful for their guidance and the opportunities they have provided me to grow and thrive in my research pursuits.

Table of Contents

<i>1. Introduction</i>	<i>1</i>
<i>1.1 Motivation</i>	<i>1</i>
<i>1.2 Microfracture</i>	<i>2</i>
<i>1.3 Fibrinogen Overview</i>	<i>5</i>
<i>1.4 The Rho/ROCK Pathway, Fasudil, and TGF-β3</i>	<i>7</i>
<i>1.5 Objectives and Significance</i>	<i>10</i>
<i>2. Materials and Methods</i>	<i>11</i>
<i>Aim 1: Developing a Fibrin-based Microfracture Clot Model</i>	<i>11</i>
<i>2.1.1 Thrombin-Mediated Gel Mechanics</i>	<i>11</i>
<i>2.1.2 Thrombin-Mediated Gel Contraction</i>	<i>12</i>
<i>2.1.3 Microscale Fiber Formation</i>	<i>12</i>
<i>2.1.4 Thrombin-Dependent Gene Expression</i>	<i>12</i>
<i>Aim 2: Microscale Cell Behavior</i>	<i>14</i>
<i>2.2.1 Fibrin Densification</i>	<i>14</i>
<i>2.2.2 Cell Mechanics</i>	<i>14</i>
<i>2.2.3 Immunofluorescence</i>	<i>15</i>
<i>Aim 3: Macroscale Clot Behavior</i>	<i>15</i>
<i>2.3.1 Macroscale Clot Contraction</i>	<i>15</i>
<i>2.3.2 Histology</i>	<i>16</i>
<i>2.3.3 Gene Expression</i>	<i>16</i>
<i>2.3.4 Statistical Analysis</i>	<i>17</i>
<i>3. Results</i>	<i>18</i>
<i>Aim 1: Developing a Fibrin-based Microfracture Clot Model</i>	<i>18</i>
<i>3.1.1 Elastic Moduli of Fibrin Gels based on Thrombin Content</i>	<i>18</i>
<i>3.1.2 Thrombin-Dependent Gel Contraction</i>	<i>19</i>
<i>3.1.3 Microscale Fiber Formation</i>	<i>20</i>
<i>3.1.4 Thrombin-Dependent Gene Expression</i>	<i>21</i>
<i>Aim 2: Microscale Cell Behavior</i>	<i>22</i>
<i>3.2.1 Fibrin Densification</i>	<i>22</i>
<i>3.2.2 Cell Mechanics</i>	<i>23</i>
<i>3.2.3 Immunofluorescence</i>	<i>24</i>
<i>Aim 3: Macroscale Clot Behavior</i>	<i>25</i>
<i>3.3.1 Macroscale Clot Contraction</i>	<i>25</i>

<i>3.3.2 Histology Images and Interpretations</i>	27
<i>3.3.3 Gene Expression</i>	28
<i>4. Discussion</i>	29
<i>5. Conclusion</i>	35
<i>Supplementary Information</i>	36
<i>References</i>	37

1. Introduction

1.1 Motivation

The bipedal gait, a distinctive characteristic of humans and our hominin ancestors, has played a pivotal role in shaping the evolution of the hominin hind limb (Darwin, 1871). Natural selection, over time, sculpted this limb to meet the biomechanical demands imposed by bipedality, significantly influencing the anatomy of the human knee (Jungers, 1988; Morrison, 1970). Recent studies suggest that chondrocyte regulatory elements may play a major role in mediating the risk of orthopedic diseases; for example, Richard *et al.* demonstrated that the genetic loci associated with chondrocyte and osteocyte development that were optimized during human knee evolution harbor an abundance of risk variants associated with osteoarthritis (OA) (Richard et al., 2020). Natural selection has clearly played a strong role in shaping knee morphology, albeit not without repercussions for human health.

Articular cartilage is the smooth, white connective tissue that lines the joints. Articular cartilage injury is one of the most prevalent connective tissue injuries and results in pain, reduced mobility, and in many cases, can progress into OA (Song & Park, 2019). OA is a degenerative joint disease that manifests as joint inflammation, stiffness, and pain. Such cartilage injuries are among the most prevalent musculoskeletal issues, with OA alone afflicting over 500 million people in 2019—an alarming 113% increase since 1990 (GBD Results, n.d.). OA presents a substantial economic burden, contributing to over \$27 billion in health care costs annually; this makes OA the second most costly health condition treated in hospitals in the United States (Guglielmo et al., 2019; *OA Prevalence and Burden - Osteoarthritis Action Alliance*, n.d.). OA prevalence is remarkably high among US military veterans compared to nonveterans, as an

alarming 35.2% of veterans report diagnosed arthritis (Fallon et al., 2023). It is also well known that OA disproportionately affects racial and ethnic minorities (Bolen et al., 2010). Despite the widespread prevalence and significant burden presented by OA, treatment options remain limited, and curative therapies have yet to be developed.

1.2 Microfracture

Given the avascular nature of cartilage, it has a limited self-regenerative capacity and is therefore unable to self-heal. Microfracture, also known as marrow stimulation, is the modern-day gold standard treatment for cartilage injuries (Fig. 1) (D'Ambrosi et al., 2018).

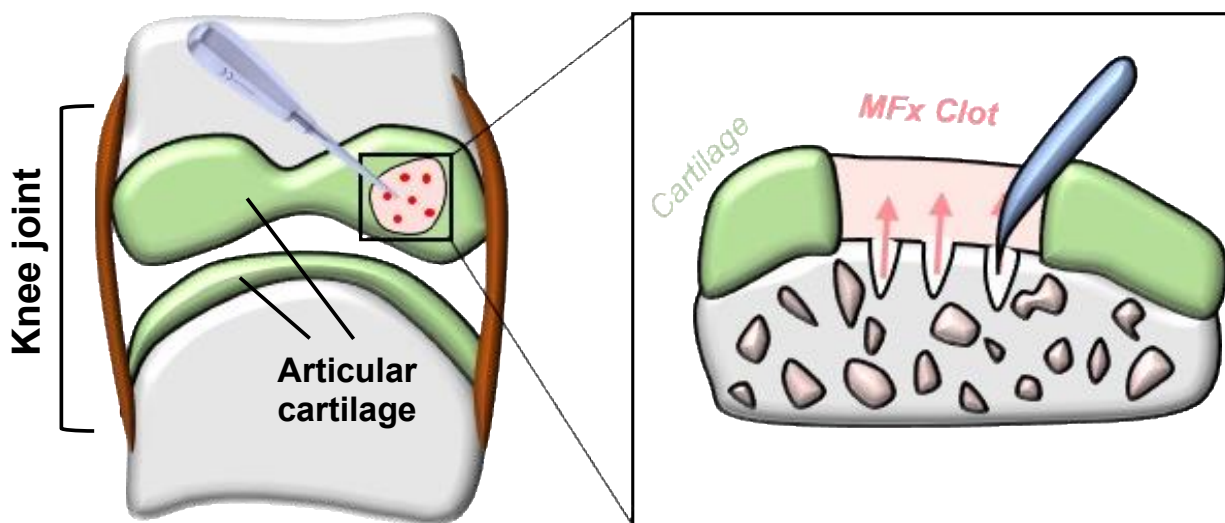


Figure 1. Schematic of microfracture (MFx) procedure.

Microfracture is a surgical technique that is implemented in patients that have developed full thickness chondral defects, wherein articular cartilage has deteriorated to the bone. The procedure consists of puncturing a small hole at the base of the cartilage injury through the subchondral bone and into the bone marrow, creating perforations 3 to 4 mm apart with an awl or drill (*Microfracture Surgery and Recovery Information*, n.d.). Bone marrow elements, including autologous mesenchymal stromal cells, are allowed to escape into the defect area. These cells are

able to fill the defect and remodel the damaged area, forming a “marrow clot” (Zlotnick et al., 2021). The theory behind this approach is to recruit the pro-regenerative cells within the marrow, namely bone marrow mesenchymal stem cells (MSCs). Microfracture is primarily performed on patients below the age of 40, as cells tend to have diminished regenerative capacity past this age (Ahmed et al., 2017; Erggelet & Vavken, 2016). Additionally, microfracture is typically only recommended for patients with a defect smaller than 2 cm² (Husen et al., 2022).

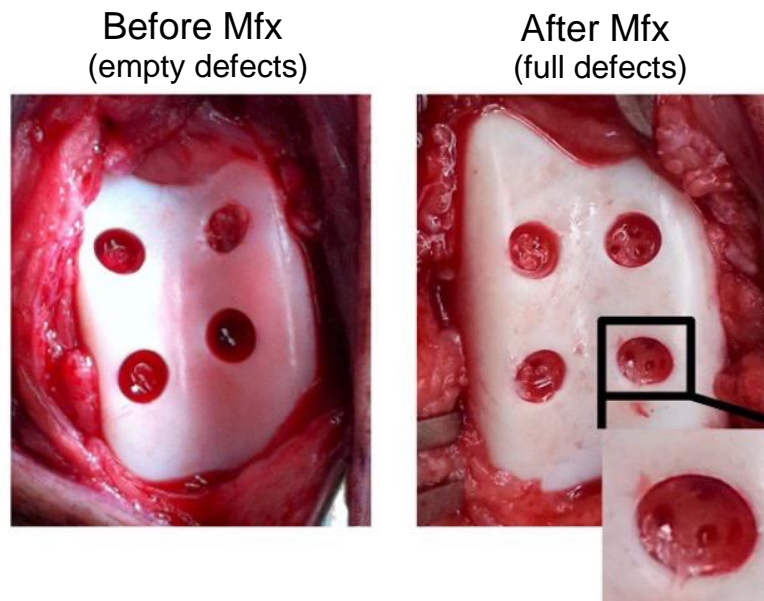


Figure 2. Photograph of microfracture procedure in Yucatan minipigs before and after perforating subchondral bone, releasing bone marrow into the defect.

Although microfracture provides short-term relief, it often leads to the formation of inferior fibrous tissue in the defect area, which has limited functional properties and is highly susceptible to wear (Welton et al., 2018). In addition, it can result in suboptimal defect filling, which leads to uneven loading and ultimately can cause progressive cartilage damage and pain (Fig. 2 and 3) (Atwal et al., 2023).

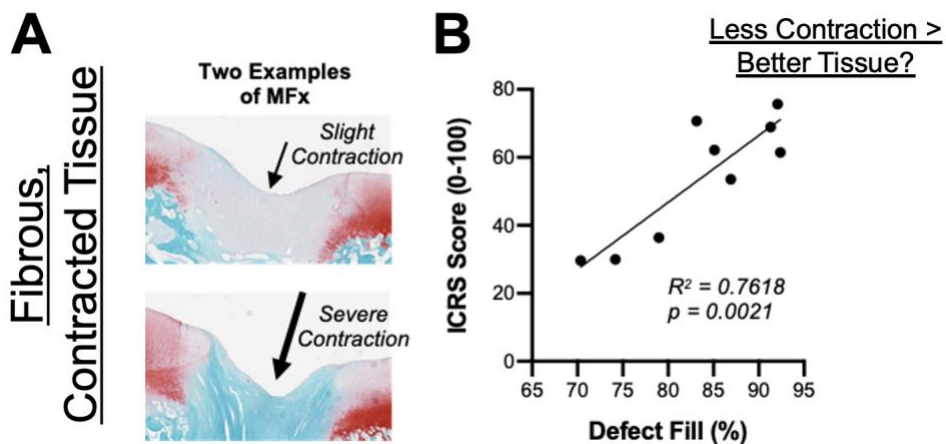


Figure 3. The development of fibrous tissue and the contraction of the defect present two major issues in microfracture repair. (A) Two Safranin-O stains of cartilage defect sites 8 weeks post-microfracture procedure in Yucatan minipigs show the development of fibrous tissue, stained white and blue, and slight and severe repair contraction. (B) International Cartilage Repair Society (ICRS) scores grade cartilage repair (100 = normal, 0 = severely abnormal). ICRS scores versus the defect fill percent reveals a positive correlation.

The limited success of marrow-derived cells alone implicates a need for better chondrogenic therapies that can augment the use of marrow cells by inducing improved chondrogenic differentiation. However, the early players in the microfracture clot, especially the initial clot structure and mechanics remain unexplored. Additionally, the microscale properties of the cells involved, particularly cellular contractility and mechanics, and the impacts of early cell behavior at on longer term cartilage healing, have not been thoroughly investigated.

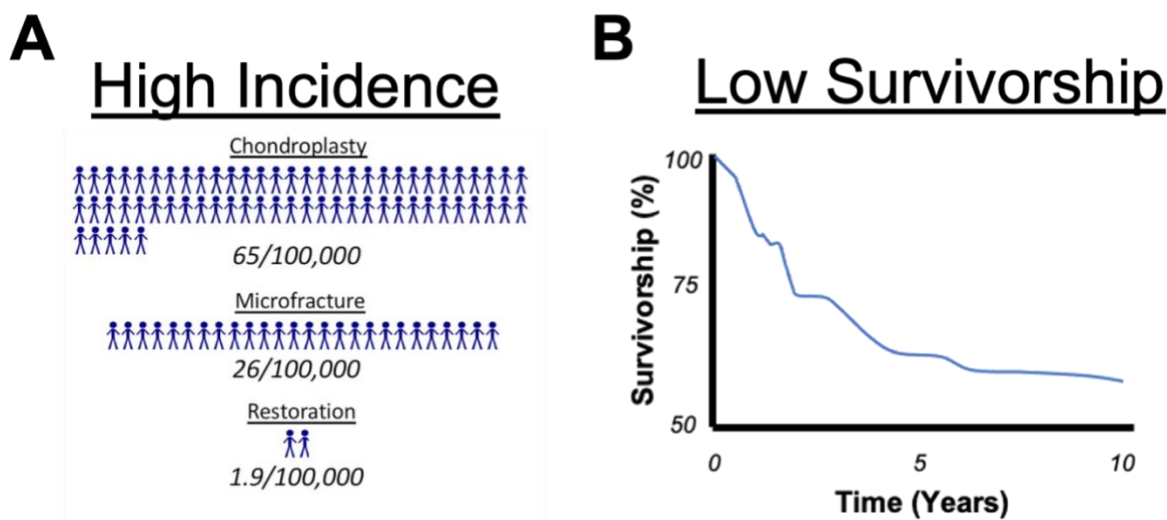


Figure 4. (A) The rate of cartilage repair procedures including chondroplasty, microfracture, and restoration per 100,000 patients annually reveals that microfracture has a relatively high incidence within the repair field (McCormick et al., 2014). Figure obtained from Martin et al. 2019 via Creative Commons License. (B) Despite this high incidence, microfracture procedures have a low survivorship, diminishing over 50% after only five years. Figure adapted from Weber et al., 2018 via Creative Commons License.

1.3 Fibrinogen Overview

Fibrinogen is a complex 340kDa hexameric plasma glycoprotein synthesized by the liver (White et al., 2023). It is soluble and present in high concentrations within blood plasma (Pieters & Wolberg, 2019). Fibrinogen plays a crucial role in blood clotting (hemostasis) by being converted into fibrin, a fibrous protein that makes up the structural basis of blood clots. When tissue injury occurs, soluble fibrinogen undergoes proteolytic cleavage by the enzyme thrombin to form insoluble fibrin strands, which aggregate to form a blood clot, preventing excess bleeding (Weisel & Litvinov, 2017). Thrombin is a serine protease enzyme involved in the coagulation cascade, and is produced from its precursor, prothrombin. It is also responsible for activating platelets and enhancing platelet aggregation, further contributing to fibrin clot formation (Di Cera, 2007). Thrombin is activated by calcium ions, which serve as a cofactor in the coagulation cascade (Fig. 5).

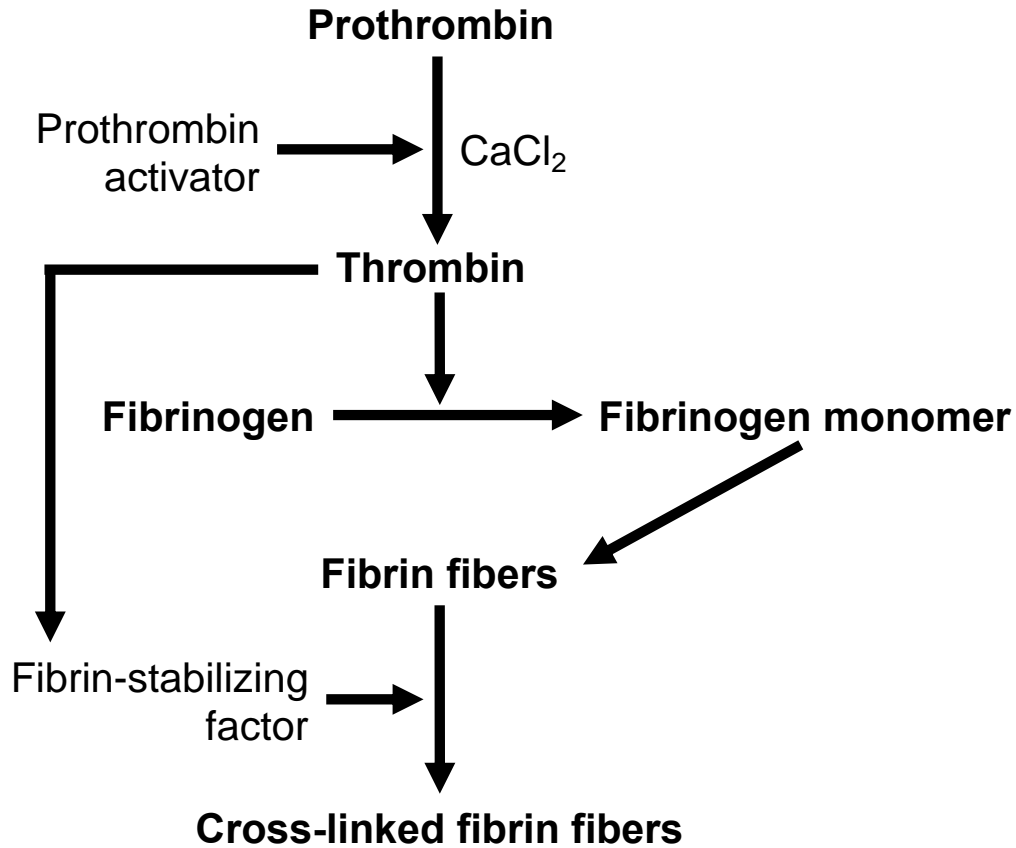


Figure 5. The conversion of fibrinogen to fibrin fibers via the action of the enzyme thrombin. Prothrombin is converted to the active enzyme thrombin using calcium ions. Thrombin is then able to cleave fibrinogen into monomers, which form fibrin strands and cross-link to form a clot. Adapted from *Guyton and Hall Textbook of Medical Physiology* (Hall, 2011).

In microfracture, the puncturing of the subchondral bone within the damaged cartilage region leads to local bleeding and subsequent formation of a fibrin clot in the defect area (Strauss et al., 2010). By creating fibrin clots in vitro using fibrinogen, thrombin, calcium chloride, and bone marrow-derived cells, this microfracture clot environment can be recapitulated, and experiments can be completed to determine the efficacy of treatments designed to augment microfracture.

1.4 The Rho/ROCK Pathway, Fasudil, and TGF- β 3

Despite its prevalence as a cartilage healing technique, microfracture procedures have many negative implications. The main goal of this thesis is to evaluate how microfracture can be augmented to resolve these issues, particularly the contraction of the microfracture defect and the fibrosis of newly synthesized tissue.

The Rho/ROCK signaling pathway is involved in various cellular processes, including cell migration, proliferation, and actin polymerization (Kim et al., 2021). The pathway is initiated by the activation of Rho GTPases, specifically RhoA, which acts as a molecular switch by cycling between an inactive GDP-bound state and an active GTP-bound state (Fig. 5). When activated, RhoA interacts with and activates its downstream effector, Rho-associated protein kinase (ROCK). ROCK is a serine/threonine kinase that is considered to be a central modulator of cytoskeletal function and affects several cellular functions, including cell motility, shape, secretion, and gene expression (Amano et al., 2010; Guan et al., 2023; Maekawa et al., 1999; McBeath et al., 2004; Riento & Ridley, 2003). ROCKs are known to induce actin reorganization, which can lead to stress fiber formation, and they are also understood to be key regulators of cellular contractility (Riento et al., 2003). Fasudil, the inhibitor used in the following studies, is a known ROCK inhibitor.

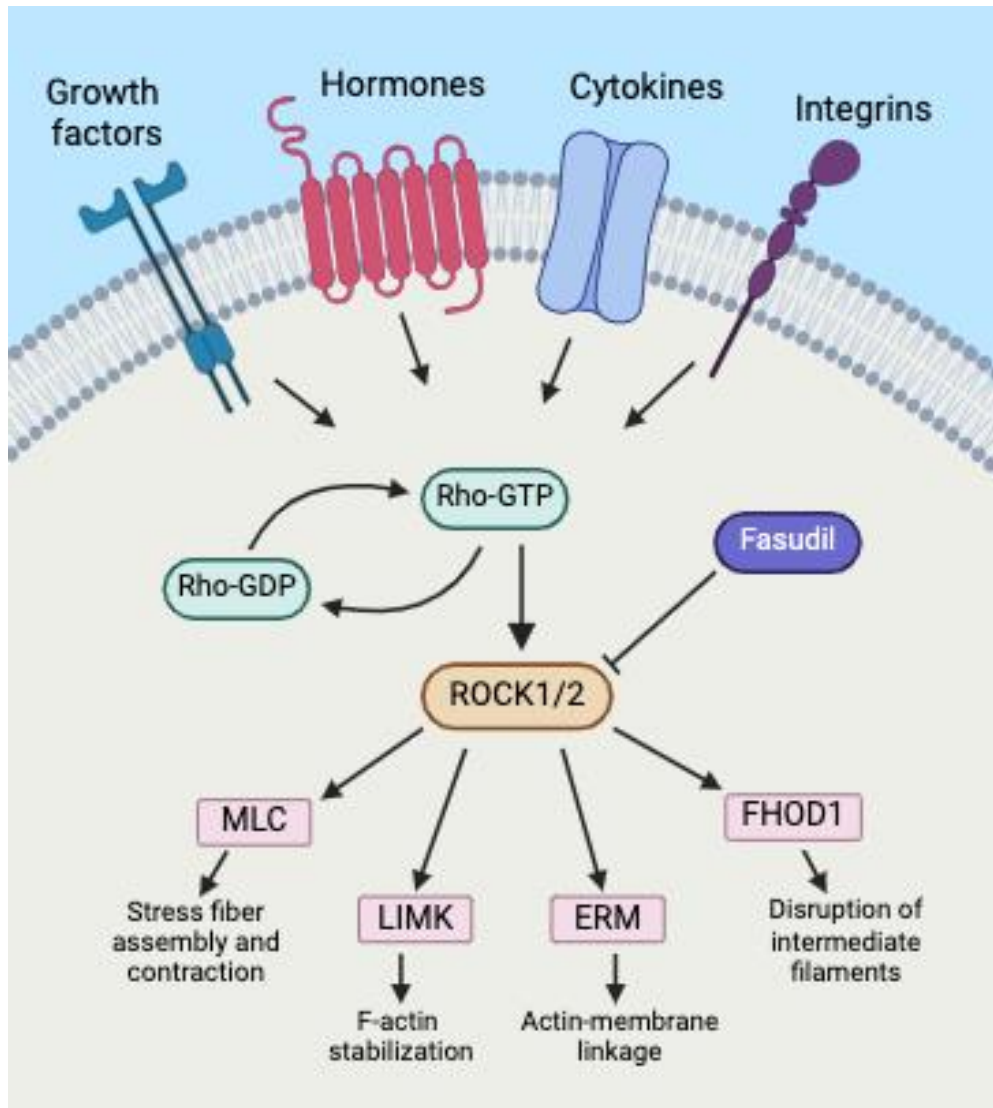


Figure 6. The Rho/ROCK pathway. GDP-bound Rho can be activated by growth factors, hormones, cytokines, and integrins, by conversion to a GTP-bound state. Rho activates ROCK1 and ROCK2, which activate and inhibit various downstream processes, including cell contraction and actin stabilization. Made using BioRender.

In the context of tissue fibrosis subsequent to microfracture procedures, bone marrow-derived cells (BMDCs) recruited into the microfracture clot undergo differentiation into fibrocartilage cells. This fibrotic cell phenotype is characterized by the formation of stress fibers, cell spreading, and down-regulated expression of SOX9, a pro-chondrogenic transcription factor, along with type-II collagen, a cartilage-specific matrix component (Benya et al., 1978; Hall,

2019). The aim of incorporating Fasudil into this project is to impede the contribution of ROCK-mediated pathways in the differentiation of MDCs into fibroblasts and redirect their differentiation towards chondrogenesis.

Transforming Growth Factor Beta 3 (TGF- β 3) is a member of the transforming growth factor beta superfamily, which includes several proteins involved in regulating various cellular processes such as cell growth, differentiation, migration, and apoptosis (Du et al., 2023). TGF- β 3 is a homodimeric protein consisting of two subunits linked by disulfide bonds. It is synthesized as an inactive precursor that requires proteolytic cleavage to become active. Once activated, TGF- β 3 binds to its receptors on the cell surface, initiating downstream signaling cascades (Heldin & Moustakas, 2016). TGF- β 3 is a known promoter of chondrogenesis, and many studies show evidence of its success as a pro-chondrogenic factor and regulator of various processes throughout the life cycle of chondrocytes (Du et al., 2023; Li et al., 2020). However, TGF- β 3 has also been implicated in joint fibrosis, which presents an issue for its use as a pharmaceutical agent for cartilage regeneration (Blaney Davidson et al., 2007; Frangogiannis, 2020; Meng et al., 2016). The goal of this project is to take advantage of the chondrogenic potential that TGF- β 3 offers while preventing its fibrosis-related side effects via ROCK inhibition.

1.5 Objectives and Significance

The goal of this thesis is to develop a fibrin gel-based microfracture model to evaluate pharmacological strategies for improving the outcomes of microfracture. I specifically hope to develop a thorough understanding of the roles of extracellular matrix organization and cell contractility in the early microfracture environment. Establishing a clearer picture of cell behavior and contraction within the microfracture clot may lead to an enhanced understanding of the fibrosis in the microfracture environment and could provide targeted pathways towards improving cartilage regeneration. Additionally, the interplay between Rho/ROCK pathway and TGF- β 3 in the early microfracture environment can help elucidate the role of cell contractility in fibrosis and may show promise as a potential therapy to treat cartilage damage as an augmentation to microfracture.

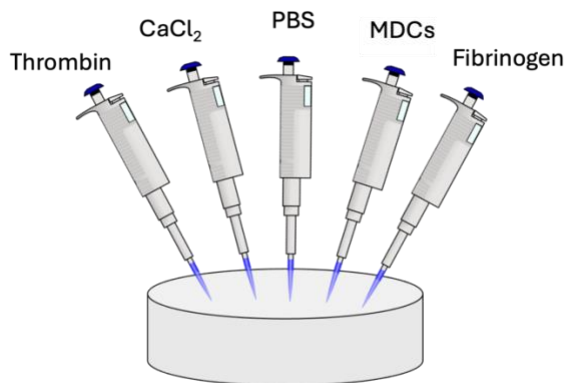
To achieve this goal, I investigated three different aims. My first aim was to develop a fibrin-based microfracture clot model. My second aim was to evaluate the influence of Rho/ROCK inhibition and TGF- β 3 stimulation by investigating microscale cell behavior. Finally, my third aim was to examine the effects of Rho/ROCK inhibition and TGF- β 3 on the macroscale clot environment by implementing Fasudil and TGF- β 3 treatment in a 3D fibrin gel. I hypothesized that Rho/ROCK inhibition would mitigate fibrosis and facilitate the maintenance of clot area, while simultaneously allowing for TGF- β 3-induced chondrogenesis.

2. Materials and Methods

Aim 1: Developing a Fibrin-based Microfracture Clot Model

2.1.1 Thrombin-Mediated Gel Mechanics

To evaluate the impact of thrombin concentration on fibrin gel mechanics, acellular fibrin gels were formulated by combining fibrinogen (50mg/mL) with a mixture of calcium chloride (10mM), PBS, and thrombin concentrations of 1, 2, 5, 10, 15, and 20 U/mL (Fig. 6). To form each gel, 50 μ L of the thrombin, calcium chloride, and PBS solution was added to each well of 96-well plate. Well plates were treated with Pluronic for one hour before adding gel solution to prevent gels from sticking to the plastic after forming. 50 μ L of fibrinogen was then added, and the solution was pipetted up and down thoroughly to mix. The resultant solution was allowed to gel at 37°C for one hour.



Microfracture clot model

Figure 7. Fibrin-based microfracture clot model schematic.

Following gelation, the gels were immersed in PBS inside of a 100mm petri dish and mechanically tested in unconfined compression between two platens to 20% strain. A total of 36 samples were tested, as six different thrombin concentrations were evaluated (n= 4 -7).

Stress/strain curves were calculated based on the platen position, corresponding force output, and

gel height, and the elastic modulus was determined by calculating the slope of the stress/strain curve.

2.1.2 Thrombin-Mediated Gel Contraction

To visualize macroscale clot contraction, fibrin clots with low and high thrombin concentrations (low = 2U/mL; high = 20U/mL) were seeded with juvenile bovine BMDCs (200 million cells per gel) before gelation. Gels were placed in 24-well plates and cultured for 4 weeks in basal media. To model the cells recruited to cartilage defects during marrow stimulation, BMDCs were isolated from juvenile bovine femoral condyles and utilized for all studies (P1-P2). The gels were imaged three times per week during feeding and at the terminal point, and clot area was subsequently quantified using FIJI to measure clot area over time.

2.1.3 Microscale Fiber Formation

To visualize thrombin-mediated clot structure, acellular 3D fibrin gels were prepared using the previously described technique, using 2 and 20U/mL of thrombin. Gels were snap-frozen in liquid nitrogen and broken in half manually to maintain internal fiber structure. The cross section of each gel was imaged using SEM.

2.1.4 Thrombin-Dependent Gene Expression

To evaluate cell behavior relative to the thrombin concentration of the fibrin gel, 3D fibrin gels were prepared using the previously defined method, containing 2, 5, 10, and 20U/mL of thrombin. Prior to gelation, gels were seeded with BMDCs (2 million cells/gel).

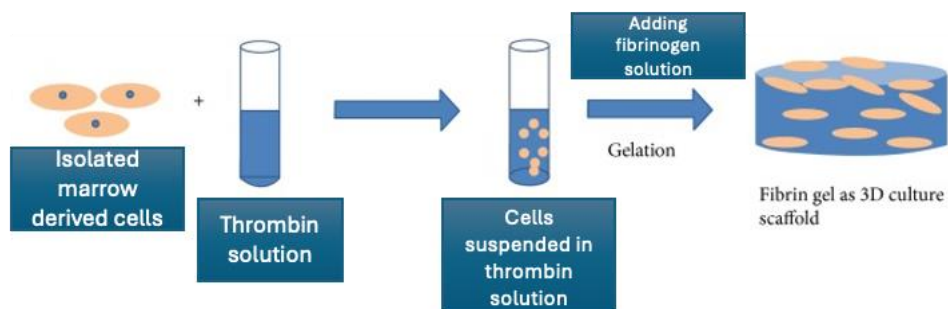


Figure 8. Formation of 3D fibrin gels containing MDCs.

After formation, gels were transferred to a 24-well plate and submerged in basal media. Gels were cultured for a four-week period. After the culture period was complete, gels were submerged in TRIzol (Thermo Fisher Scientific), placed over ice, and homogenized in 2mL tubes. Chloroform (200 μ L/mL) was added to each gel solution to initiate phase separation, and the solution was gently inverted before incubating at room temperature for five minutes. Solutions were spun at 12000xg for 15 minutes, and the aqueous layer was carefully pipetted into a separate 1.5mL tube. This solution was mixed with equal parts of 75% ethanol, and the resulting solution was added to RNA columns and re-spun for two minutes. This process was repeated using a low stringency buffer solution, a high stringency buffer solution, and an elution solution to isolate the washed RNA. Next, RNA content and quality was quantified using a Nanodrop. Following RNA isolation, cDNA was synthesized using the calculated quantities of RNA, as well as DI water and a prepared cDNA mix (SuperScript). Relative real-time RT-PCR was performed using equal concentrations of cDNA. In 96-well PCR plates, cDNA was combined with PowerUp SYBR Green qPCR Master Mix (Thermo Fisher Scientific), DI water, and primers for beta actin (housekeeping gene) and Acta2 (smooth muscle actin). Plates were run in a PCR machine and relative gene expression was determined using the outputted CT values relative to beta actin content. All final gene expression values were normalized to the control.

Aim 2: Microscale Cell Behavior

2.2.1 Fibrin Densification

To understand the early micro-scale contraction and densification of fibrin clots in response to Rho/ROCK inhibition, we used a 2D fibrin gel model with fluorescently labeled fibrinogen. Fibrinogen (final concentration: 5mg/mL) labeled with CruzFluor 405 (1% w/w) was mixed with thrombin (1-5U/mL) and calcium chloride (20mM) in an 8-chamber slide and allowed to gel for 60 minutes. BMDCs (1500/gel) were then seeded on top of gels, and the constructs were cultured for 24 hours in basal media or media containing 50 μ M of Fasudil (Rho/ROCK inhibitor). Samples were fixed using 4% paraformaldehyde and stained using Phalloidin 555, a peptide that stains actin filaments. Samples were imaged using a confocal microscope (Nikon A1R) to visualize the contracting fibrin network and actin densification surrounding the cells.

2.2.2 Cell Mechanics

To evaluate the influence of Fasudil and TGF- β 3 on cellular mechanical properties, MDCs were cultured in basal media (10% FBS, 1% PSF) in 6-well plates for three days, after which the media was replaced with basal media containing Fasudil (Fas; Rho-ROCK inhibitor; 50 μ M) and/or TGF- β 3 (10ng/mL) for 45 minutes. Individual cell mechanics were measured using image-guided nanoindentation (Optics 11 Pavone; 3 μ m radius probe), and load-deformation curves were used to obtain Effective Young's modulus.

2.2.3 Immunofluorescence

To assess the impact of inhibiting Rho/ROCK on nuclear SMAD 2/3 activity, MDCs were cultured in basal media in an 8-well chamber slide for three days. The media was then replaced with chemically defined media (CDM) or CDM containing Fasudil for 24 hours. TGF- β 3 (10ng/mL) was then applied for 60 minutes, and cells were fixed using 4% paraformaldehyde and stained for SMAD 2/3 (TGF- β 3 activation), SMA (stress fiber formation) and phalloidin (F-Actin visualization). Cells were imaged using confocal microscopy (Nikon A1R) and analyzed for nuclear SMAD 2/3 intensity and actin/SMA colocalization. Quantification of nuclear SMAD 2/3 intensity was calculated using the negative log of nuclear to perinuclear SMAD 2/3 intensity.

Aim 3: Macroscale Clot Behavior

2.3.1 Macroscale Clot Contraction

To visualize macroscale clot contraction, 3D fibrin gels were prepared using the previously mentioned techniques (50mg/mL fibrinogen, 10U/mL thrombin) and were seeded with juvenile bovine MDCs (2M/mL) before gelation. They were cultured for four weeks in basal media or media containing Fasudil. Initially, two different Fasudil concentrations were tested for dose-dependence (10 μ M and 50 μ M). For future studies, 50 μ M was selected for use, and gels were tested after a four-week culture period in basal media, 50 μ M Fasudil media, TGF- β 3 (10ng/mL) media, and Fasudil/TGF- β 3 media. Clots were imaged three times per week and at the final time point to determine contraction over time. After the culture period, the constructs were harvested for histology and gene expression.

2.3.2 Histology

After a four-week culture, gels were fixed in 4% paraformaldehyde for 30 minutes and rinsed in PBS before being set in OCT within plastic molds. Gels were set at room temperature for 2 hours and then allowed to freeze at -20°C . Constructs were then sectioned to a width of $10\mu\text{m}$ and mounted on slides. Sections were stained using a Safranin-O/Fast green stain. Safranin-O is a red dye that stains proteoglycans, a major component of ECM in articular cartilage. The intensity of the red Safranin-O stain is proportional to the proteoglycan content in the tissue of interest. Fast green is a counter stain often used to supplement Safranin-O and stains collagen fibers and cytoplasmic components. Safranin-O/Fast green stains provide a means of evaluating fibrin gel structure and degradation, as well as matrix deposition in response to pharmacological treatments.

Gel sections were rinsed in DI water and fast green (0.05%) was applied for three minutes. They were then submerged in 1% acetic acid for 10 seconds, followed by 0.2% Safranin O for 15 minutes. Next, sections were rinsed and dehydrated using ethanol and xylene, and set using Permount. Sections were then imaged at 10X using light microscopy (Echo).

2.3.3 Gene Expression

After 4 weeks in culture, gels were submerged in TRIzol (Thermo Fisher Scientific), placed over ice, and homogenized in 2mL tubes. RNA isolation, cDNA preparation, and RT-PCR was completed using the aforementioned technique. Gene expression for beta actin and type-II collagen was evaluated. All final gene expression values were normalized to the control.

2.3.4 Statistical Analysis

All data was subject to outlier (ROUT method). Parametric, normal datasets were analyzed with a one-way analysis of variance (ANOVA) with post-hoc Tukey's testing. Nonparametric or non-normal datasets were analyzed with a KruskalWallis test with post-hoc Dunn's Multiple Comparison Test. All data are shown as dot plots for transparency, and $p < 0.05$ was chosen as a threshold for statistical significance.

3. Results

Aim 1: Developing a Fibrin-based Microfracture Clot Model

3.1.1 Elastic Moduli of Fibrin Gels based on Thrombin Content

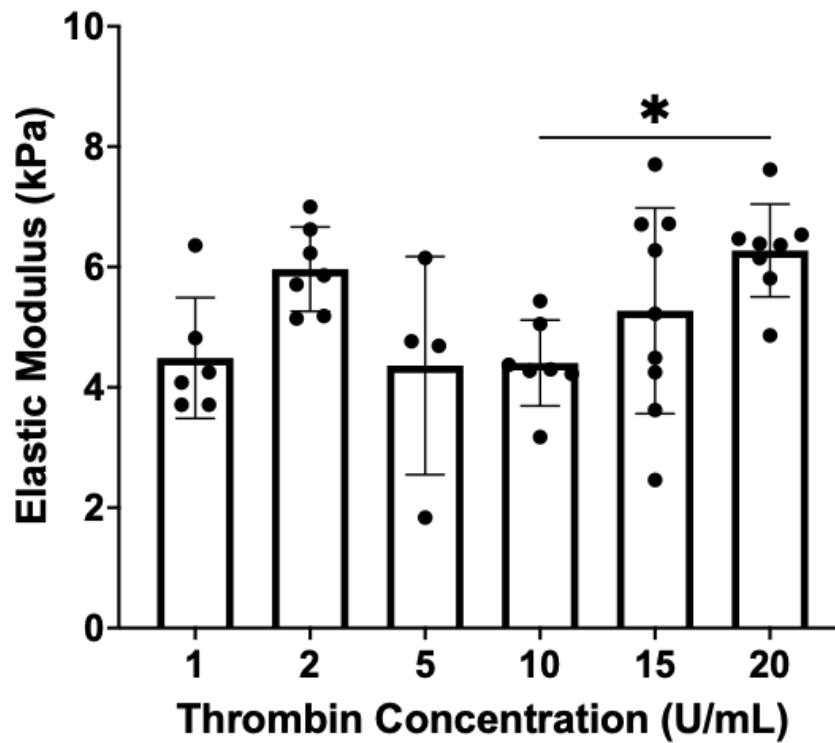


Figure 9. Elastic moduli of fibrin gels relative to thrombin concentration (n values range from 3 to 7; * P-value = 0.0128).

Elastic modulus, measured in kilopascals, is indicative of a substance's resistance to deformation, and is calculated based on a ratio of stress to strain. Higher elastic moduli represent gels that are stiffer, or more resistant to this deformation, and lower elastic moduli represent softer gels. The initial gel environment aims to represent cartilage, a very stiff material, so ideal elastic moduli for this structure should be relatively high (stiff). Mechanical testing revealed a nonlinear trend in the elastic moduli of fibrin clots with varied thrombin concentrations,

generally increasing from 5-20 U/mL of thrombin but peaking at 2 and 20 U/mL of thrombin (Fig. 9).

3.1.2 Thrombin-Dependent Gel Contraction

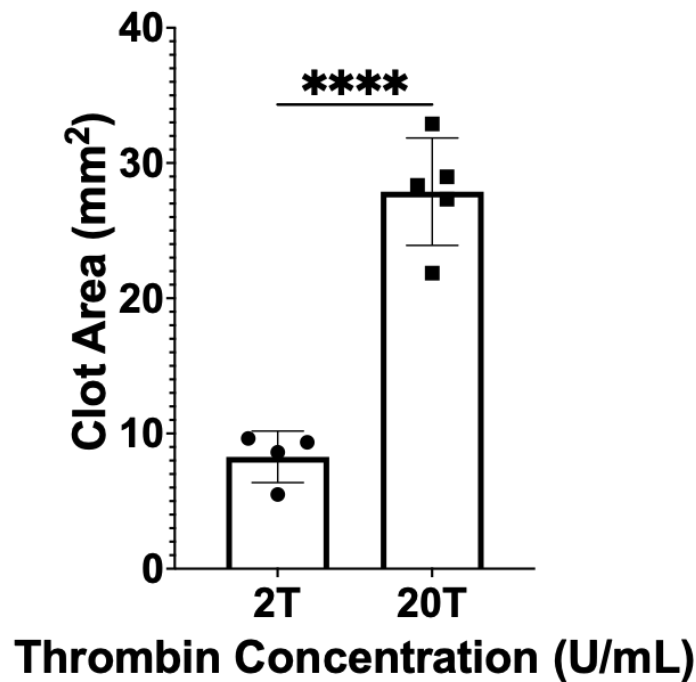


Figure 10. Final area of high (20U/mL) and low (2U/mL) thrombin clot models after four weeks in culture (n = 4-5). Low thrombin clots contracted to below 10mm², whereas high thrombin clots maintained nearly three times this area. ****P-value<0.0001

The mechanical testing results implicated the 2 and 20U/mL thrombin gels as the more resistant to deformation; based on these outcomes, these thrombin concentrations were further assessed to evaluate differences in contraction over time. Contraction of the microfracture defect is a significant issue in tissue repair, so improved therapies should seek to limit or mitigate contraction levels. After culturing fibrin gels (containing 2 and 20 U/mL of thrombin) over a four-week period, the low-thrombin gel experienced significant contraction, whereas the high-thrombin gel maintained a larger area (Fig. 10).

3.1.3 Microscale Fiber Formation

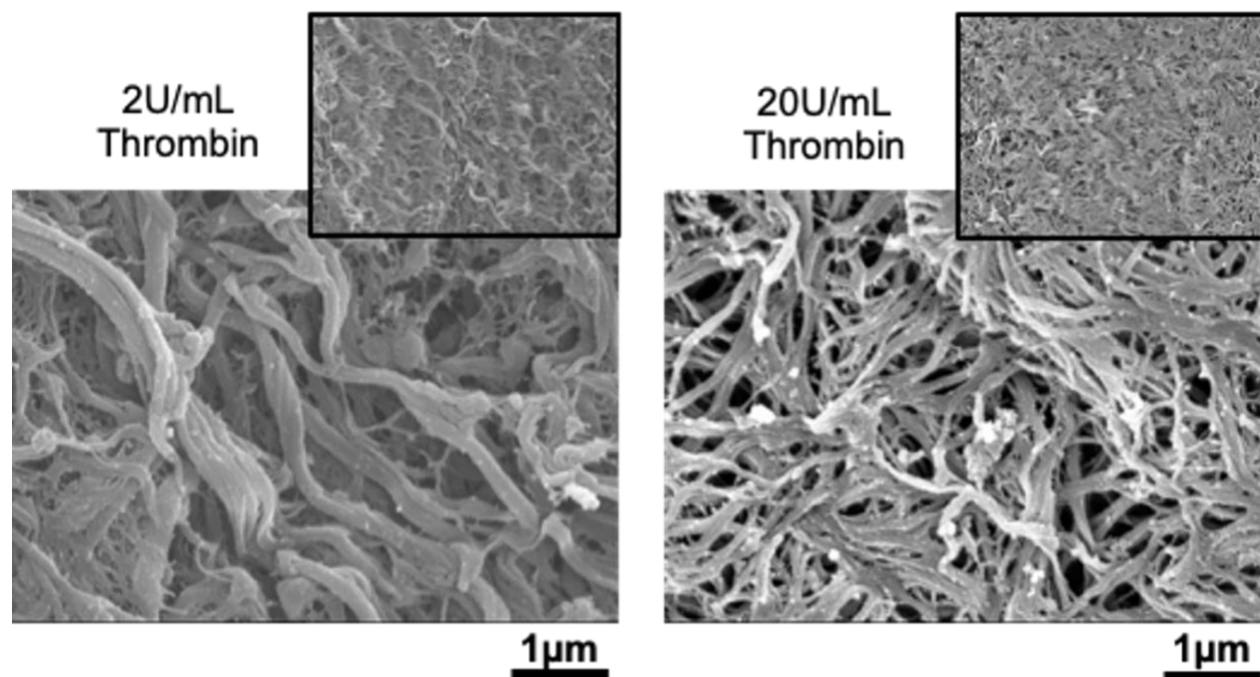


Figure 11. SEM images of acellular thrombin gels for structural comparison.

Despite having similar elastic moduli, the high and low thrombin gels exhibited remarkably different levels of contraction over time. This led us to evaluate gel structure on a microscale, to determine if fiber organization may play a role in this behavior. SEM imaging revealed that the low-thrombin gels exhibited thicker fibrin fibers, whereas high-thrombin gels yielded thinner fibers (Fig. 11).

3.1.4 Thrombin-Dependent Gene Expression

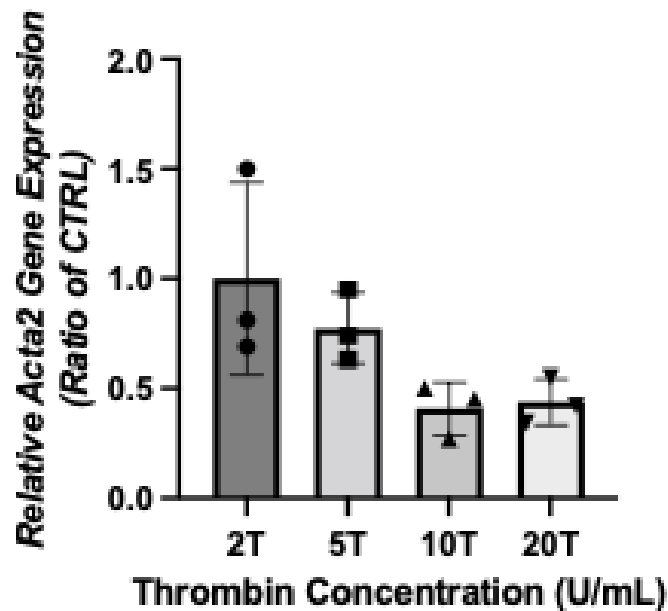


Figure 12. Gene expression of Acta2 (n = 3; 2U/mL vs 10U/mL P-value = 0.0718; 2U/mL vs 20U/mL P-value= 0.0886).

Acta2 is the gene that provides instructions for making smooth muscle actin, which is a type of actin that is typically implicated in fibrotic cell phenotypes. Increased levels of Acta2 are indicative of fibrosis; tissue fibrosis is one of the negative consequences of microfracture that this study aims to target. Gene expression of gels with varied thrombin concentration revealed that cells within fibrin gels of lower thrombin concentrations express more Acta2 compared to cells within high thrombin gel environments (Fig. 12). Acta2 expression was highest in the 2U/mL thrombin group and decreased to similar levels in 10 and 20U/mL groups.

Aim 2: Microscale Cell Behavior

3.2.1 Fibrin Densification

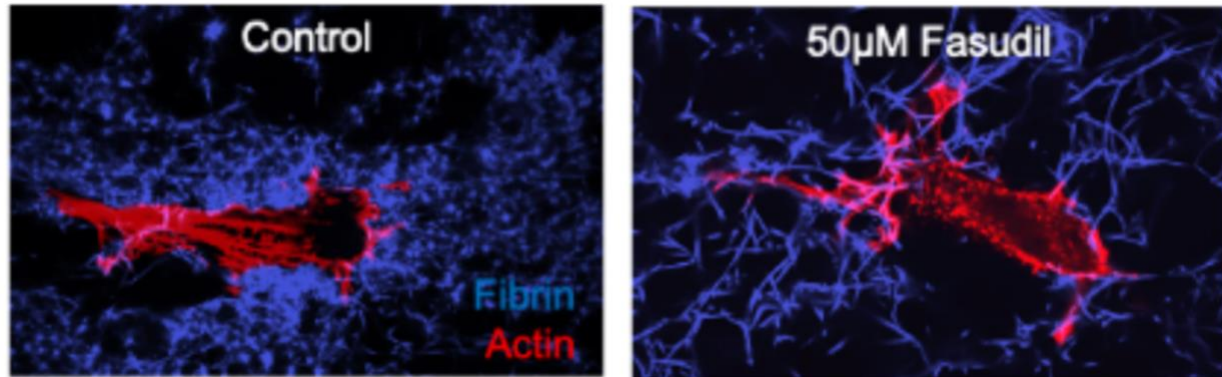


Figure 13. Microscale images of cells on 2D gels showed that 50uM Fasudil-treated gels showed less actin stress fibers (red) and less fibrin densification (blue) than cells cultured in control media.

To holistically understand the microscale environment of cells following microfracture procedures, it was initially necessary to evaluate the cell's interaction with its immediate environment: the fibrin gel. In this study, I evaluated how this interaction differed with the addition of Fasudil. Confocal microscopy images of MDCs seeded on top of 2D fibrin gels exhibited differences in fibrin densification surrounding the cell as well as the organization of actin within the cell (Fig. 13). Cells treated with Fasudil have fewer stress fibers compared to the control, and the structure of the fibrin gel that is in direct contact with the cell is much less dense, indicating that the cell is not contracting within the gel and pulling the fibrin fibers towards itself and therefore Fasudil treatment is effectively reducing cell contractility.

3.2.2 Cell Mechanics

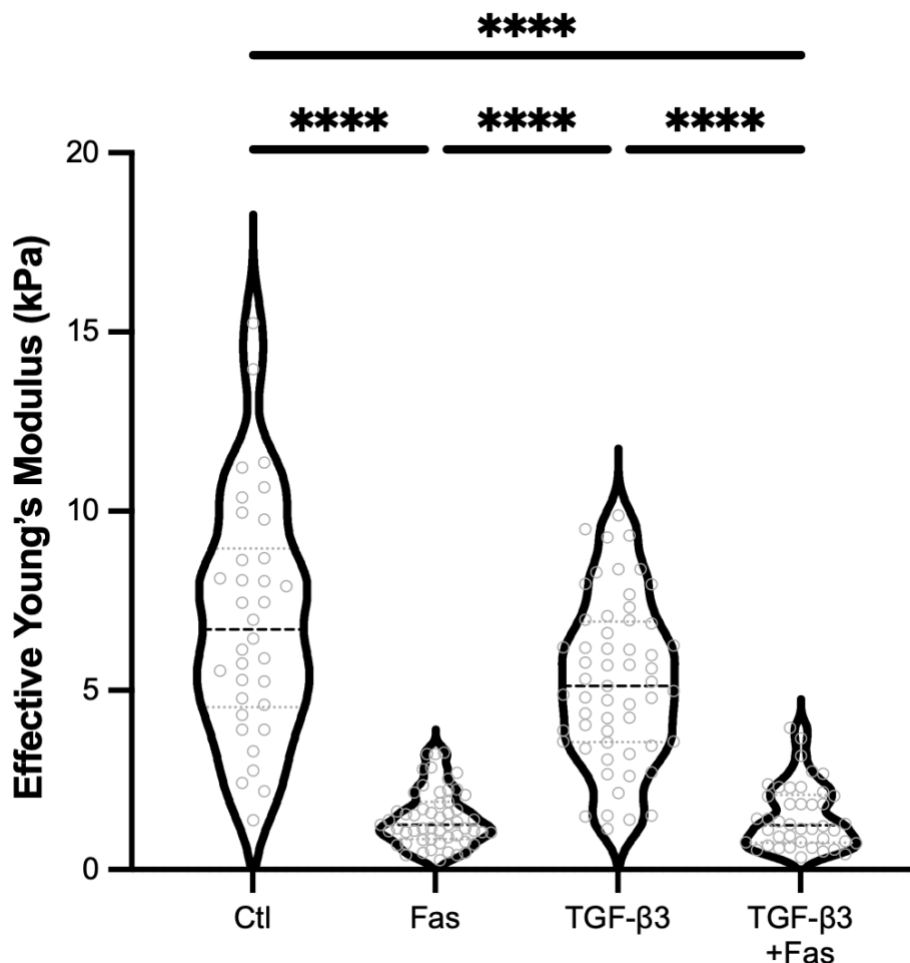


Figure 14. Effect Young's Modulus of individual MDCs treated with basal media (control), Fasudil (50 μ M) and/or TGF- β 3 (10ng/mL) for 45 minutes (n = 43-57). ****P-value<0.0001

Nanoindentation studies revealed that cells treated with Fasudil experienced a significant reduction in Effective Young's Modulus compared to the control group (Fig. 14). Cells treated with TGF- β 3 exhibited a slight decrease in modulus compared to the control, but the same significant reduction in modulus was observed with the addition of Fasudil to TGF- β 3-treated cells.

3.2.3 Immunofluorescence

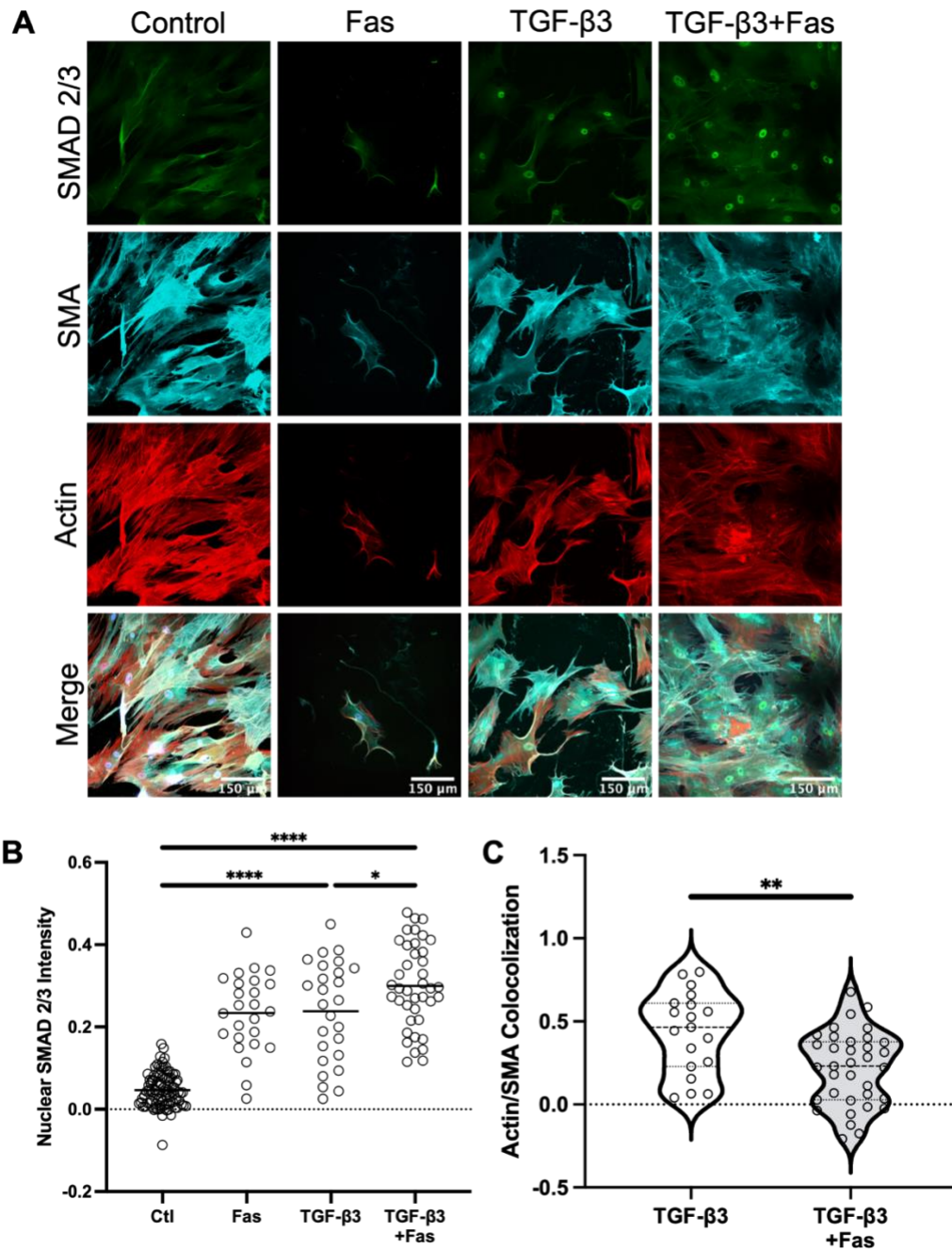


Figure 15. (A) Immunofluorescent staining of MDCs on glass cultured in basal media, Fasudil media (50 μ M), TGF- β 3 media (10ng/mL), and Fasudil/ TGF- β 3 media. SMAD 2/3 is green, smooth muscle actin (SMA) is cyan, actin is red, and actin/SMA overlap is white. (B) Quantification of nuclear SMAD 2/3 intensity using the negative log of the ratio of nuclear to perinuclear intensity (n = 25-95). ****P-value<0.0001, *P-value = 0.0133 (C) Quantification of stress fibers based on Actin/SMA colocalization (n = 19-35). **P-value=0.0018

Quantification of immunofluorescence staining for SMAD 2/3 revealed enhanced nuclear localization of SMAD 2/3 in TGF- β 3 treated cells compared to the control, and an even greater increase in groups co-treated with both TGF- β 3 and Fasudil (Fig. 15A and B). Quantification of actin/SMA colocalization revealed that Fasudil treatment significantly reduced stress fiber formation in cells treated with TGF- β 3 (Fig. 15C).

Aim 3: Macroscale Clot Behavior

3.3.1 Macroscale Clot Contraction

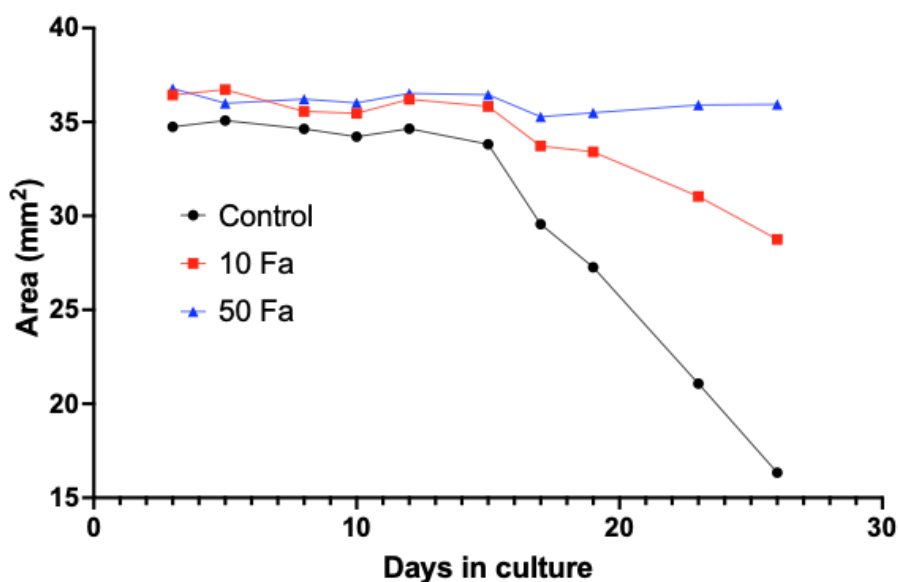


Figure 16. Dose-dependent contraction of clots after four weeks in culture. Clots cultured in basal media (control) contracted significantly after four weeks, whereas Fasudil treatment mitigated contraction in a dose-dependent manner.

After tracking the contraction of gels over time, it was observed that area begins to decrease substantially around the two-week timepoint. By the end of the four-week culture period, control gels had significantly contracted. Gels cultured in 10 μ M Fasudil contracted slightly, however not as much as the control group, and gels cultured in 50 μ M Fasudil barely experienced any difference in area compared to the initial time point (Fig. 16). Based on these

results, it is clear that Fasudil treatment plays a role in macroscale contraction, and acts in a dose-dependent manner.

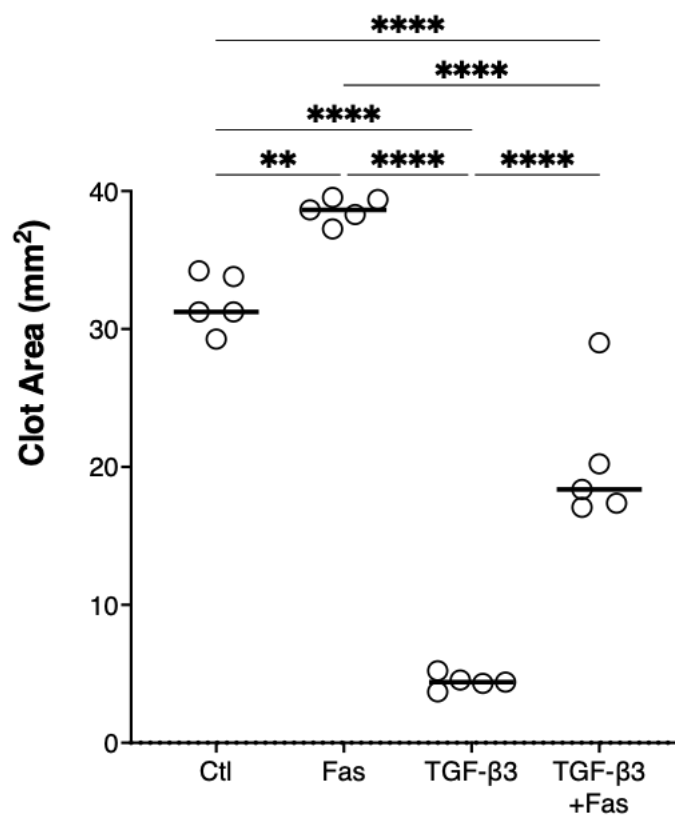


Figure 17. Final area of fibrin clots after four weeks in culture containing basal media (Ctl), Fasudil (Fas; 50 μ M), TGF- β 3 (10ng/mL), and TGF- β 3 + Fasudil (n = 5). ****P-value<0.0001, **P-value<0.01

Area quantification of fibrin clots after a 4-week culture period in control and Fasudil and/or TGF- β 3 media revealed that Fasudil-treated gels experienced no contraction over time, whereas TGF- β 3 treated gels contracted significantly (Fig. 17). Co-treated gels contracted less than TGF- β 3 treated gels, indicating that Fasudil prevented gel contraction by a significant amount.

3.3.2 Histology Images and Interpretations

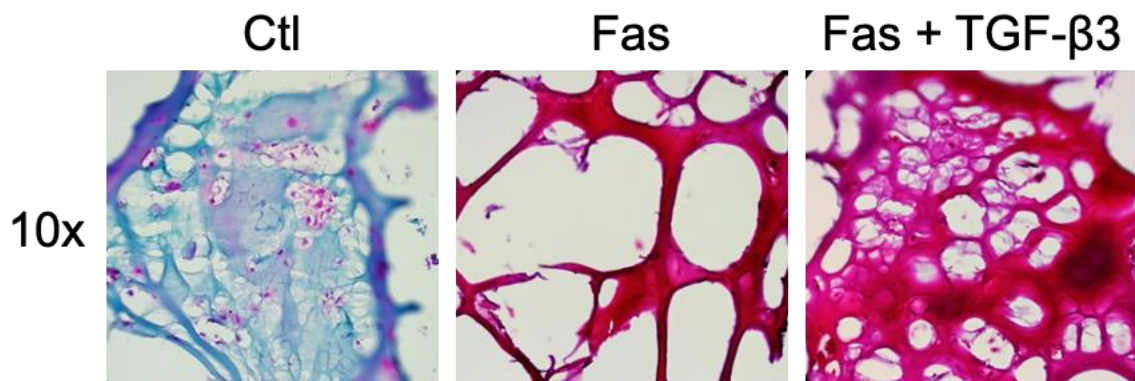


Figure 18. Safranin-O/Fast green staining of control (Ctl), Fasudil (Fas; 50 μ M), and TGF- β 3 (10ng/mL) + Fasudil-treated clots after four weeks. Red = Safranin-O, blue = Fast green.

Safranin-O staining revealed that Fasudil and TGF- β 3 + Fasudil treated gels exhibited considerably enhanced proteoglycan deposition compared to the control. Furthermore, the gels that were treated with Fasudil alone appeared much less dense than the control gels, indicating that cells treated with TGF- β 3 deposit more matrix components and maintain a denser structure throughout the treatment period (Fig. 18). Gels treated with TGF- β 3 alone were excluded from this study due to excessive contraction at the terminal timepoint.

3.3.3 Gene Expression

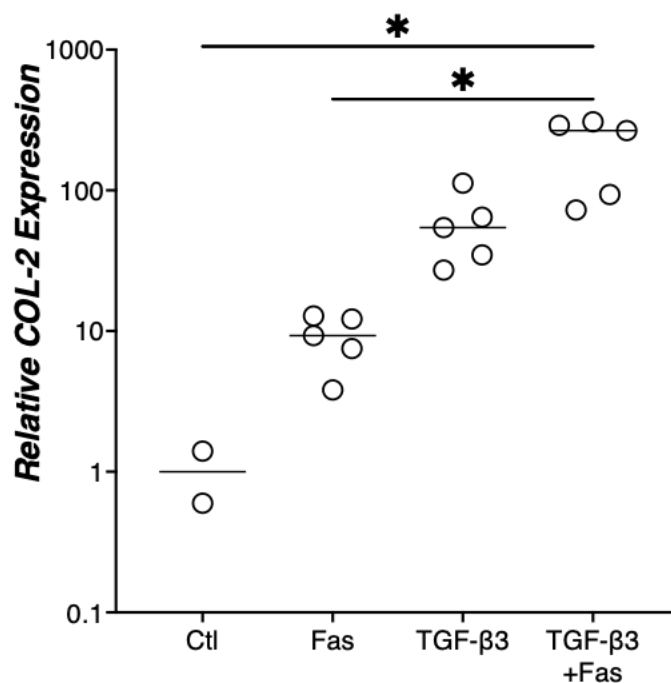


Figure 19. Relative type-II collagen expression of control (Ctl), Fasudil (Fas; 50 μ M), TGF- β 3 and TGF- β 3 (10ng/mL) + Fasudil-treated clots after four weeks (n = 2-5). *P-value<0.05

Type-II collagen is an ECM component found in high amounts in native cartilage, and is indicative of pro-chondrogenic differentiation. Gene expression results revealed that TGF- β 3 and Fasudil treatment increased type-II collagen expression after four weeks in culture (Fig. 19). The Fasudil-alone group increased type-II collagen expression by a roughly 9-fold increase, whereas the Fasudil + TGF- β 3 group experienced nearly a 200-fold increase in type-II collagen expression compared to the control.

4. Discussion

To develop an *in vitro* model of the microfracture clot using fibrin gels, it is important to first understand the composition and structure of the gel, especially as it pertains to contraction. We investigated this by altering thrombin concentration within the gels and measuring mechanical properties, contraction and gene expression, as well as evaluating the structure visually through SEM. The results of our analysis of thrombin concentration revealed that the microscale properties of the microfracture clot, specifically the fiber thickness and porosity of the fibrin network, may have a significant impact on macroscale clot contraction over time. Thrombin concentrations of 2 and 20 U/mL seemed to produce the stiffest fibrin gels, however once cultured, it was found that the gels containing 2 U/mL of thrombin contracted significantly more than the 20 U/mL gels. This indicates that, despite sharing similar bulk mechanical properties, the fibrin network is altered such that the lower thrombin gels are more prone to contraction over time.

SEM images of the two clot structures revealed remarkable differences in fiber formation; the low thrombin concentration gel consisted of thicker, less densely packed fibrin fibers, whereas its high thrombin counterpart was constructed of thinner, more concentrated fibers. This marked difference in gel structure may explain the observed difference in contraction: gels that are densely packed with fibrin fibers may present more resistance to contraction compared to gels that are loosely constructed. This investigation of the fibrin gel microenvironment is currently ongoing; the rest of this project serves to elucidate the cell's perception of this environment and how it can be altered.

After evaluating the structural properties of the clot, we conducted a deeper exploration of cell behavior by evaluating Rho/ROCK inhibition with the addition of TGF- β 3. The inhibition of Rho/ROCK altered fibrin densification surrounding cells within this microenvironment. When

Fasudil was added to a 2D fibrin gel environment, microscale images revealed less fibrin densification around MDCs compared to gels in control media, indicating that Fasudil may be preventing cells from contracting their surrounding environment. The visualization of stress fibers, a phenotypic marker of cell fibrosis, also decreased with the addition of Fasudil, implicating Fasudil as a potential anti-fibrotic factor.

We evaluated cell stiffness via nanoindentation to assess force generation, and we visualized cell markers of TGF- β 3 activation and fibrosis. Nanoindentation studies revealed that Fasudil treatment significantly decreased Effective Young's Modulus, and this effect was maintained when Fasudil was added in addition to TGF- β 3. These results demonstrate that Rho/ROCK inhibition greatly reduces the cell's generation of force, even when applied in addition to a growth factor. Next, nuclear SMAD 2/3 was evaluated. SMAD 2 and 3 are core transcription factors that are involved in TGF- β signaling; an intense nuclear SMAD 2/3 stain indicates that the cell is responding to the growth factor (*SMAD2 SMAD Family Member 2 [Homo Sapiens (Human)] - Gene - NCBI*, n.d.). As anticipated, cells treated with TGF- β 3 alone exhibited enhanced nuclear SMAD 2/3 intensity. Interestingly, when treated with both Fasudil and TGF- β 3, cells exhibited an even greater response to TGF- β 3 as demonstrated by enhanced SMAD 2/3 nuclear intensity, indicating that Rho-ROCK inhibition improves early TGF- β 3 activation of the SMAD 2/3 pathway. Furthermore, Fasudil treatment decreased the development of stress fibers in TGF- β 3 treated cells, indicating that Rho-ROCK inhibition plays a role in preventing MDCs from attaining fibrotic morphologies.

The final goal of this project was to implement Fasudil and TGF- β 3 treatments in the context of a 3D fibrin gel. Macroscale clot behavior was assessed by measuring gel contraction, histology for proteoglycan deposition, and gene expression for type-II collagen. Dose-

dependency studies illustrated that 50 μ M Fasudil media mitigated contraction to the highest extent compared to 10 μ M doses, and therefore future work proceeded using the 50 μ M dose. Macroscale studies revealed that Rho/ROCK inhibition greatly mitigated gel contraction in TGF- β 3 -treated gels, indicating that Fasudil treatment prevents contraction of the gel on a macroscale level and therefore may aid in maintaining the fill of microfracture repair.

Histology results showed that Fasudil treatment alone promotes proteoglycan deposition but increases gel porosity after four weeks in culture. Combined treatment with TGF- β 3 both enhanced proteoglycan deposition and maintained clot density, which would allow for the development of more condensed, structured, cartilage-like tissue in the microfracture defect. Furthermore, gene expression studies showed that Fasudil and TGF- β 3 treatment significantly enhanced the expression of type-II collagen, a known marker of chondrogenesis, over four weeks. The combined effects of Rho/ROCK inhibition and TGF- β 3 suggest that Fasudil treatment would help maintain defect fill while simultaneously promoting cartilage regeneration. Exploring the interplay between the Rho/ROCK pathway and TGF- β 3 could potentially provide a deeper insight into strategies for fostering chondrogenesis following marrow stimulation while maintaining the volume of the repair tissue.

While this project offers valuable insights into augmenting the microfracture repair environment, several limitations should be acknowledged. Firstly, all studies were done using juvenile bovine-derived cells. Although many cell properties are conserved between human and bovine cells, there may be subtle differences in their responses to the aforementioned treatments. It is also notable that these cells were juvenile; younger cells are understood to have a higher regenerative capacity than older cells, so when implemented in adults, the observed effects may

not be as extreme (Yun, 2015). We are currently working on replicating these results using cells derived from adult human donors.

It is also necessary to address donor dependence. Variability in donor characteristics such as age, sex, and health status could potentially confound our results, leading to limitations in the generalizability and reproducibility of our findings. Future studies could address this by incorporating a larger and more diverse donor pool. Lastly, our experimental design involved the use of cells harvested from bone marrow, which has a notoriously heterogeneous cell population, comprising various cell subtypes with potentially distinct characteristics (Baccin et al., 2020; Peci et al., 2022a, 2022b; Yu & Scadden, 2016). While this approach aimed to capture the complexity of the cellular landscape involved in microfracture, it also introduces challenges in interpreting and extrapolating our findings. The presence of diverse cell types within the population could lead to variability in experimental outcomes, making it challenging to discern specific cellular responses. Furthermore, differences in the proportions of cell subtypes across experimental replicates or conditions may contribute to variability in data interpretation and limit the reproducibility of our results. Future studies could address these limitations by employing more homogeneous cell populations or utilizing advanced techniques such as single-cell sequencing to dissect the contributions of individual cell types to observed phenotypes, thus enhancing the precision and validity of our conclusions.

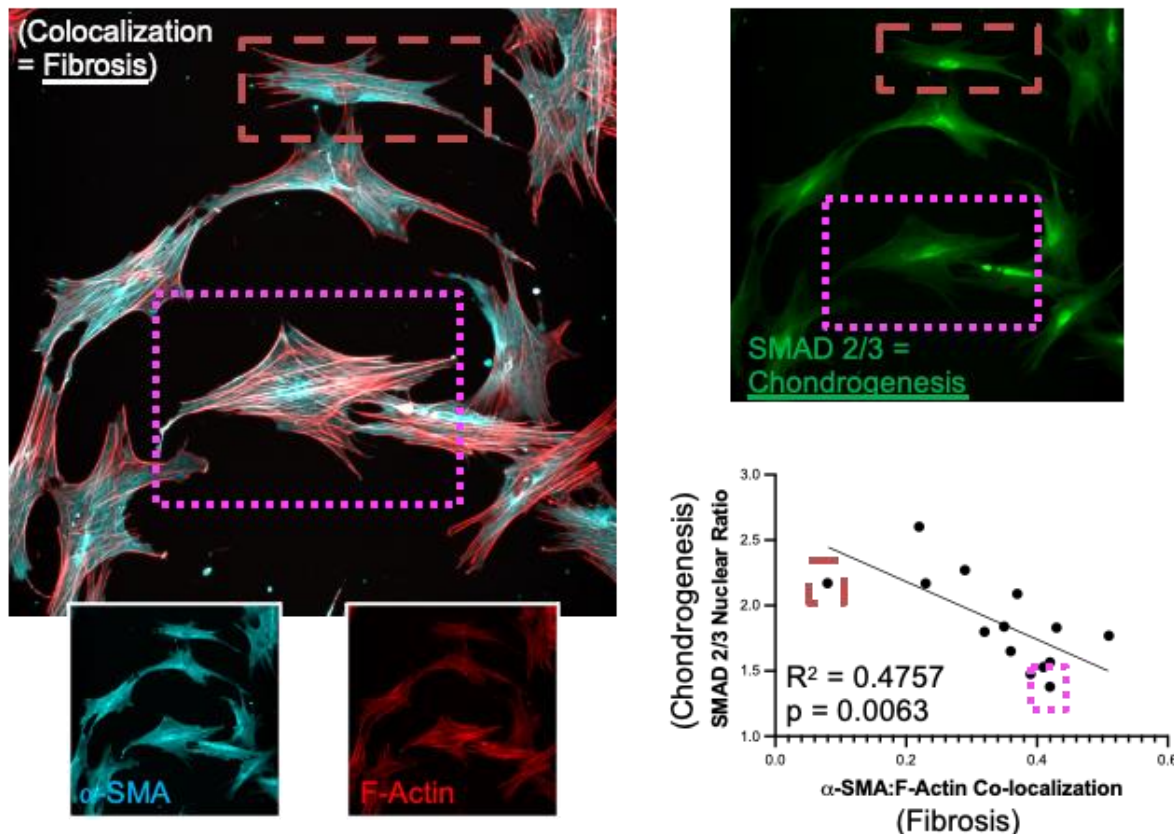


Figure 120. Visualization of the Fibro-Chondro Axis, a proposed method for evaluating cell propensities towards fibrosis and chondrogenesis based on early cell markers (SMA/Actin colocalization represents a fibrotic cell marker, and SMAD 2/3 nuclear intensity represents a pro-chondrogenic cell marker). This axis could be used as a predictive measure to screen patients' future repair outcomes at an earlier timepoint.

Moving forward, our study lays the groundwork for several promising avenues of research. The translation of our findings into an animal model system could provide valuable insights into the efficacy of Fasudil and TGF- β 3 co-treatment in a more complex biological context. Furthermore, future studies should aim to delineate a clearer relationship between early markers of fibrosis and chondrogenesis and their markers at later timepoints to construct a predictive framework for long-term outcomes (Fig. 20). By systematically tracking the trajectory of treatment responses over time, we can better understand the dynamic nature of disease progression and identify early markers that correlate with favorable or adverse outcomes. This

predictive model could inform clinical decision-making and facilitate personalized treatment strategies tailored to individual patient needs. Overall, the integration of animal modeling and longitudinal analyses holds promise for advancing our understanding of disease mechanisms and optimizing therapeutic interventions for improved patient outcomes.

5. Conclusion

This study demonstrates that altering microscale properties of microfracture clots, such as fiber thickness and porosity, significantly affects macroscale clot contraction, potentially impacting early microfracture healing. Moreover, Rho/ROCK inhibition with Fasudil influences cell behavior and mechanics, particularly in conjunction with TGF- β 3, enhancing chondrogenesis and preventing fibrotic morphologies. Overall, these findings suggest that targeting the Rho/ROCK pathway, in combination with TGF- β 3, could improve cartilage regeneration and defect fill following marrow stimulation, providing valuable insights for augmenting microfracture repair.

Supplementary Information

Abbreviations List:

TGF- β 3 = Transforming Growth Factor Beta 3

SMA = Smooth Muscle Actin

OA = Osteoarthritis

CaCl₂ = Calcium Chloride

Ca = Calcium

w/v = Weight per Volume

ROCK = Rho-associated Protein Kinase

COL-2 = Type-II Collagen

MDC = Marrow-derived Cell

MFx = Microfracture

BMDC = Bone Marrow-derived Cell

MSC = Mesenchymal Stromal Cell

PBS = Phosphate Buffered Saline

kPa= Kilopascal

SEM = Scanning Electron Microscopy

RNA = Ribonucleic Acid

cDNA = Complementary Deoxyribonucleic Acid

DI = Deionized

OCT = Optimal Cutting Temperature

CDM = Chemically Defined Media

ECM = Extracellular Matrix

ROUT = Regression and Outlier

ANOVA = Analysis of Variance

References

- Ahmed, A. S. I., Sheng, M. H., Wasnik, S., Baylink, D. J., & Lau, K.-H. W. (2017). Effect of aging on stem cells. *World Journal of Experimental Medicine*, 7(1), 1–10.
<https://doi.org/10.5493/wjem.v7.i1.1>
- Akiyama, H. (2008). Control of chondrogenesis by the transcription factor Sox9. *Modern Rheumatology*, 18(3), 213–219. <https://doi.org/10.1007/s10165-008-0048-x>
- Amano, M., Nakayama, M., & Kaibuchi, K. (2010). Rho-Kinase/ROCK: A Key Regulator of the Cytoskeleton and Cell Polarity. *Cytoskeleton (Hoboken, N.j.)*, 67(9), 545–545.
<https://doi.org/10.1002/CM.20472>
- Atwal, A., Dale, T. P., Snow, M., Forsyth, N. R., & Davoodi, P. (2023). Injectable hydrogels: An emerging therapeutic strategy for cartilage regeneration. *Advances in Colloid and Interface Science*, 321, 103030–103030. <https://doi.org/10.1016/J.CIS.2023.103030>
- Baccin, C., Al-Sabah, J., Velten, L., Helbling, P. M., Grünschläger, F., Hernández-Malmierca, P., Nombela-Arrieta, C., Steinmetz, L. M., Trumpp, A., & Haas, S. (2020). Combined single-cell and spatial transcriptomics reveals the molecular, cellular and spatial bone marrow niche organization. *Nature Cell Biology*, 22(1), 38–38. <https://doi.org/10.1038/S41556-019-0439-6>
- Benya, P. D., Padilla, S. R., & Nimni, M. E. (1978). Independent regulation of collagen types by chondrocytes during the loss of differentiated function in culture. *Cell*, 15(4), 1313–1321.
[https://doi.org/10.1016/0092-8674\(78\)90056-9](https://doi.org/10.1016/0092-8674(78)90056-9)
- Blaney Davidson, E. N., van der Kraan, P. M., & van den Berg, W. B. (2007). TGF- β and osteoarthritis. *Osteoarthritis and Cartilage*, 15(6), 597–604.
<https://doi.org/10.1016/J.JOCA.2007.02.005>
- Bolen, J., Schieb, L., Hootman, J. M., Helmick, C. G., Theis, K., Murphy, L. B., & Langmaid, G. (2010). Peer Reviewed: Differences in the Prevalence and Impact of Arthritis Among

Racial/Ethnic Groups in the United States, National Health Interview Survey, 2002, 2003, and 2006. *Preventing Chronic Disease*, 7(3), 1–5.

Bryant, J., Yi, P., Miller, L., Peek, K., & Lee, D. (2018). Potential Sex Bias Exists in Orthopaedic Basic Science and Translational Research. *JBJS*, 100(2), 124.

<https://doi.org/10.2106/JBJS.17.00458>

D'Ambrosi, R., Ragone, V., & Ursino, N. (2018). What future in the treatment of osteochondral knee defects? *Annals of Translational Medicine*, 6(Suppl 2), S100–S100.

<https://doi.org/10.21037/ATM.2018.11.28>

Darwin, C. R. (1871). *The descent of man, and selection in relation to sex* (1st ed., Vol. 1). John Murray. <https://darwin->

[online.org.uk/content/frameset?pageseq=1&itemID=F937.1&viewtype=text](https://darwin-online.org.uk/content/frameset?pageseq=1&itemID=F937.1&viewtype=text)

Darwin, C. R. 1871. The descent of man, and selection in relation to sex. London: John Murray. Vol.

1. (n.d.). Retrieved December 7, 2023, from <http://darwin->

[online.org.uk/content/frameset?pageseq=1&itemID=F937.1&viewtype=text](http://darwin-online.org.uk/content/frameset?pageseq=1&itemID=F937.1&viewtype=text)

Di Cera, E. (2007). Thrombin as procoagulant and anticoagulant. *Journal of Thrombosis and Haemostasis*, 5(SUPPL. 1), 196–202. <https://doi.org/10.1111/J.1538-7836.2007.02485.X>

Du, X., Cai, L., Xie, J., & Zhou, X. (2023). The role of TGF-beta3 in cartilage development and osteoarthritis. *Bone Research*, 11(1). <https://doi.org/10.1038/S41413-022-00239-4>

Erggelet, C., & Vavken, P. (2016). Microfracture for the treatment of cartilage defects in the knee joint—A golden standard? *Journal of Clinical Orthopaedics and Trauma*, 7(3), 145–152.

<https://doi.org/10.1016/j.jcot.2016.06.015>

- Fallon, E. A., Boring, M. A., Foster, A. L., Stowe, E. W., Lites, T. D., & Allen, K. D. (2023). Arthritis Prevalence Among Veterans—United States, 2017–2021. *MMWR. Morbidity and Mortality Weekly Report*, 72(45), 1209–1216. <https://doi.org/10.15585/MMWR.MM7245A1>
- Frangogiannis, N. G. (2020). Transforming growth factor- β in tissue fibrosis. *The Journal of Experimental Medicine*, 217(3). <https://doi.org/10.1084/JEM.20190103>
- Freemont, A. J., & Hoyland, J. (2006). Lineage plasticity and cell biology of fibrocartilage and hyaline cartilage: Its significance in cartilage repair and replacement. *European Journal of Radiology*, 57(1), 32–36. <https://doi.org/10.1016/j.ejrad.2005.08.008>
- GBD Results*. (n.d.). Institute for Health Metrics and Evaluation. Retrieved December 7, 2023, from <https://vizhub.healthdata.org/gbd-results>
- Geller, S. E., Koch, A., Pellettieri, B., & Carnes, M. (2011). Inclusion, Analysis, and Reporting of Sex and Race/Ethnicity in Clinical Trials: Have We Made Progress? *Journal of Women's Health*, 20(3), 315–320. <https://doi.org/10.1089/jwh.2010.2469>
- Guan, G., Cannon, R. D., Coates, D. E., & Mei, L. (2023). Effect of the Rho-Kinase/ROCK Signaling Pathway on Cytoskeleton Components. *Genes*, 14(2). <https://doi.org/10.3390/GENES14020272>
- Guglielmo, D., Murphy, L. B., Boring, M. A., Theis, K. A., Helmick, C. G., Hootman, J. M., Odom, E. L., Carlson, S. A., Liu, Y., Lu, H., & Croft, J. B. (2019). State-Specific Severe Joint Pain and Physical Inactivity Among Adults with Arthritis—United States, 2017. *MMWR. Morbidity and Mortality Weekly Report*, 68(17), 381–387. <https://doi.org/10.15585/MMWR.MM6817A2>
- Hall, A. C. (2019). The Role of Chondrocyte Morphology and Volume in Controlling Phenotype—Implications for Osteoarthritis, Cartilage Repair, and Cartilage Engineering. *Current Rheumatology Reports*, 21(8). <https://doi.org/10.1007/S11926-019-0837-6>

- Hall, J.E. (2011). Hemostasis and blood coagulation. In *Guyton and Hall Textbook of Medical Physiology* (12th ed., pp. 457–459). Elsevier Health Sciences.
- Heldin, C. H., & Moustakas, A. (2016). Signaling Receptors for TGF- β Family Members. *Cold Spring Harbor Perspectives in Biology*, 8(8). <https://doi.org/10.1101/CSHPERSPECT.A022053>
- Husen, M., Custers, R. J. H., Hevesi, M., Krych, A. J., & Saris, D. B. F. (2022). Size of cartilage defects and the need for repair: A systematic review. *Journal of Cartilage & Joint Preservation*, 2(3), 100049. <https://doi.org/10.1016/j.jcjp.2022.100049>
- Jungers, W. L. (1988a). Relative joint size and hominoid locomotor adaptations with implications for the evolution of hominid bipedalism. *Journal of Human Evolution*, 17(1–2), 247–265. [https://doi.org/10.1016/0047-2484\(88\)90056-5](https://doi.org/10.1016/0047-2484(88)90056-5)
- Jungers, W. L. (1988b). Relative joint size and hominoid locomotor adaptations with implications for the evolution of hominid bipedalism. *Journal of Human Evolution*, 17(1), 247–265. [https://doi.org/10.1016/0047-2484\(88\)90056-5](https://doi.org/10.1016/0047-2484(88)90056-5)
- Katz, J. N., Wright, E. A., Guadagnoli, E., Liang, M. H., Karlson, E. W., & Cleary, P. D. (1994). Differences between men and women undergoing major orthopedic surgery for degenerative arthritis. *Arthritis and Rheumatism*, 37(5), 687–694. <https://doi.org/10.1002/art.1780370512>
- Kim, S., Kim, S. A., Han, J., & Kim, I. S. (2021). Rho-Kinase as a Target for Cancer Therapy and Its Immunotherapeutic Potential. *International Journal of Molecular Sciences*, 22(23). <https://doi.org/10.3390/IJMS222312916>
- Korf-Klingebiel, M., Kempf, T., Sauer, T., Brinkmann, E., Fischer, P., Meyer, G. P., Ganser, A., Drexler, H., & Wollert, K. C. (2008). Bone marrow cells are a rich source of growth factors and cytokines: Implications for cell therapy trials after myocardial infarction. *European Heart Journal*, 29(23), 2851–2858. <https://doi.org/10.1093/eurheartj/ehn456>

Li, D., Ma, X., & Zhao, T. (2020). Mechanism of TGF- β 3 promoting chondrogenesis in human fat stem cells. *Biochemical and Biophysical Research Communications*, 530(4), 725–731.

<https://doi.org/10.1016/J.BBRC.2020.06.147>

Maekawa, M., Ishizaki, T., Boku, S., Watanabe, N., Fujita, A., Iwamatsu, A., Obinata, T., Ohashi, K., Mizuno, K., & Narumiya, S. (1999). Signaling from Rho to the actin cytoskeleton through protein kinases ROCK and LIM-kinase. *Science (New York, N.Y.)*, 285(5429), 895–898.

<https://doi.org/10.1126/SCIENCE.285.5429.895>

Martín, A. R., Patel, J. M., Zlotnick, H. M., Carey, J. L., & Mauck, R. L. (2019). Emerging therapies for cartilage regeneration in currently excluded ‘red knee’ populations. *Npj Regenerative Medicine*, 4(1), 1–11. <https://doi.org/10.1038/s41536-019-0074-7>

McBeath, R., Pirone, D. M., Nelson, C. M., Bhadriraju, K., & Chen, C. S. (2004). Cell shape, cytoskeletal tension, and RhoA regulate stem cell lineage commitment. *Developmental Cell*, 6(4), 483–495. [https://doi.org/10.1016/S1534-5807\(04\)00075-9](https://doi.org/10.1016/S1534-5807(04)00075-9)

McCormick, F., Harris, J. D., Abrams, G. D., Frank, R., Gupta, A., Hussey, K., Wilson, H., Bach, B., & Cole, B. (2014). Trends in the surgical treatment of articular cartilage lesions in the United States: An analysis of a large private-payer database over a period of 8 years. *Arthroscopy: The Journal of Arthroscopic & Related Surgery: Official Publication of the Arthroscopy Association of North America and the International Arthroscopy Association*, 30(2), 222–226.

<https://doi.org/10.1016/j.arthro.2013.11.001>

Microfracture Surgery and Recovery Information. (n.d.).

[https://www.ortho.wustl.edu/content/Patient-Care/2893/Services/Sports-](https://www.ortho.wustl.edu/content/Patient-Care/2893/Services/Sports-Medicine/Overview/Knee/Microfracture.aspx)

[Medicine/Overview/Knee/Microfracture.aspx](https://www.ortho.wustl.edu/content/Patient-Care/2893/Services/Sports-Medicine/Overview/Knee/Microfracture.aspx)

- Morrison, J. B. (1970a). The mechanics of the knee joint in relation to normal walking. *Journal of Biomechanics*, 3(1), 51–61. [https://doi.org/10.1016/0021-9290\(70\)90050-3](https://doi.org/10.1016/0021-9290(70)90050-3)
- Morrison, J. B. (1970b). The mechanics of the knee joint in relation to normal walking. *Journal of Biomechanics*, 3(1), 51–61. [https://doi.org/10.1016/0021-9290\(70\)90050-3](https://doi.org/10.1016/0021-9290(70)90050-3)
- OA Prevalence and Burden—Osteoarthritis Action Alliance. (n.d.). <https://oaaction.unc.edu/oa-module/oa-prevalence-and-burden/>
- Peci, F., Dekker, L., Pagliaro, A., van Boxtel, R., Nierkens, S., & Belderbos, M. (2022a). The cellular composition and function of the bone marrow niche after allogeneic hematopoietic cell transplantation. *Bone Marrow Transplantation* 2022 57:9, 57(9), 1357–1364. <https://doi.org/10.1038/s41409-022-01728-0>
- Peci, F., Dekker, L., Pagliaro, A., van Boxtel, R., Nierkens, S., & Belderbos, M. (2022b). The cellular composition and function of the bone marrow niche after allogeneic hematopoietic cell transplantation. *Bone Marrow Transplantation* 2022 57:9, 57(9), 1357–1364. <https://doi.org/10.1038/s41409-022-01728-0>
- Pieters, M., & Wolberg, A. S. (2019). Fibrinogen and fibrin: An illustrated review. *Research and Practice in Thrombosis and Haemostasis*, 3(2), 161–161. <https://doi.org/10.1002/RTH2.12191>
- Richard, D., Liu, Z., Cao, J., Kiapour, A. M., Willen, J., Yarlagadda, S., Jagoda, E., Kolachalama, V. B., Sieker, J. T., Chang, G. H., Muthuirulan, P., Young, M., Masson, A., Konrad, J., Hosseinzadeh, S., Maridas, D. E., Rosen, V., Krawetz, R., Roach, N., & Capellini, T. D. (2020a). Evolutionary Selection and Constraint on Human Knee Chondrocyte Regulation Impacts Osteoarthritis Risk. *Cell*, 181(2), 362–381.e28. <https://doi.org/10.1016/J.CELL.2020.02.057>
- Richard, D., Liu, Z., Cao, J., Kiapour, A. M., Willen, J., Yarlagadda, S., Jagoda, E., Kolachalama, V. B., Sieker, J. T., Chang, G. H., Muthuirulan, P., Young, M., Masson, A., Konrad, J.,

- Hosseinzadeh, S., Maridas, D. E., Rosen, V., Krawetz, R., Roach, N., & Capellini, T. D. (2020b). Evolutionary Selection and Constraint on Human Knee Chondrocyte Regulation Impacts Osteoarthritis Risk. *Cell*, *181*(2), 362–381.e28. <https://doi.org/10.1016/j.cell.2020.02.057>
- Riento, K., Guasch, R. M., Garg, R., Jin, B., & Ridley, A. J. (2003). RhoE Binds to ROCK I and Inhibits Downstream Signaling. *Molecular and Cellular Biology*, *23*(12), 4219–4219. <https://doi.org/10.1128/MCB.23.12.4219-4229.2003>
- Riento, K., & Ridley, A. J. (2003). Rocks: Multifunctional kinases in cell behaviour. *Nature Reviews. Molecular Cell Biology*, *4*(6), 446–456. <https://doi.org/10.1038/NRM1128>
- ROCK Signaling Pathway—Creative Diagnostics*. (n.d.). Retrieved March 18, 2024, from <https://www.creative-diagnostics.com/rock-signaling-pathway.htm>
- SMAD2 SMAD family member 2 [Homo sapiens (human)]—Gene—NCBI*. (n.d.). <https://www.ncbi.nlm.nih.gov/gene/4087>
- Song, S. J., & Park, C. H. (2019). Microfracture for cartilage repair in the knee: Current concepts and limitations of systematic reviews. *Annals of Translational Medicine*, *7*(Suppl 3), S108–S108. <https://doi.org/10.21037/ATM.2019.05.11>
- Strauss, E. J., Barker, J. U., Kercher, J. S., Cole, B. J., & Mithoefer, K. (2010). Augmentation Strategies following the Microfracture Technique for Repair of Focal Chondral Defects. *Cartilage*, *1*(2), 145–145. <https://doi.org/10.1177/1947603510366718>
- Tarr, B. (2017). Social Bonding Through Dance and ‘Musiking.’ In N. J. Enfield & P. Kockelman (Eds.), *Distributed Agency* (p. 0). Oxford University Press. <https://doi.org/10.1093/acprof:oso/9780190457204.003.0016>
- Weber, A. E., Locker, P. H., Mayer, E. N., Cvetanovich, G. L., Tilton, A. K., Erickson, B. J., Yanke, A. B., & Cole, B. J. (2018). Clinical Outcomes After Microfracture of the Knee: Midterm

Follow-up. *Orthopaedic Journal of Sports Medicine*, 6(2), 2325967117753572.

<https://doi.org/10.1177/2325967117753572>

Wei, Y., Luo, L., Gui, T., Yu, F., Yan, L., Yao, L., Zhong, L., Yu, W., Han, B., Patel, J. M., Liu, J. F.,

Beier, F., Levin, L. S., Nelson, C., Shao, Z., Han, L., Mauck, R. L., Tsourkas, A., Ahn, J., ...

Qin, L. (2021). Targeting cartilage EGFR pathway for osteoarthritis treatment. *Science*

Translational Medicine, 13(576), eabb3946. <https://doi.org/10.1126/scitranslmed.abb3946>

Weisel, J. W., & Litvinov, R. I. (2017). Fibrin Formation, Structure and Properties. *Sub-Cellular*

Biochemistry, 82, 405–405. https://doi.org/10.1007/978-3-319-49674-0_13

Welton, K. L., Logterman, S., Bartley, J. H., Vidal, A. F., & McCarty, E. C. (2018). Knee Cartilage

Repair and Restoration: Common Problems and Solutions. *Clinics in Sports Medicine*, 37(2),

307–330. <https://doi.org/10.1016/J.CSM.2017.12.008>

White, N. J., Gonzalez, E., Moore, E. E., & Moore, H. B. (2023). Fibrinogen. *Trauma Induced*

Coagulopathy, 101–116. https://doi.org/10.1007/978-3-030-53606-0_8

Woods, A., Wang, G., & Beier, F. (2005). RhoA/ROCK signaling regulates Sox9 expression and

actin organization during chondrogenesis. *The Journal of Biological Chemistry*, 280(12), 11626–

11634. <https://doi.org/10.1074/jbc.M409158200>

Yu, V. W. C., & Scadden, D. T. (2016). Heterogeneity of the Bone Marrow Niche. *Current Opinion*

in Hematology, 23(4), 331–331. <https://doi.org/10.1097/MOH.0000000000000265>

Yun, M. H. (2015). Changes in Regenerative Capacity through Lifespan. *International Journal of*

Molecular Sciences, 16(10), 25392–25392. <https://doi.org/10.3390/IJMS161025392>

Zeigler, A. C., Richardson, W. J., Holmes, J. W., & Saucerman, J. J. (2016). Computational modeling

of cardiac fibroblasts and fibrosis. *Journal of Molecular and Cellular Cardiology*, 93, 73–83.

<https://doi.org/10.1016/j.yjmcc.2015.11.020>

Zlotnick, H. M., Locke, R. C., Stoeckl, B. D., Patel, J. M., Gupta, S., Browne, K. D., Koh, J., Carey, J.

L., & Mauck, R. L. (2021). Marked differences in local bone remodelling in response to different marrow stimulation techniques in a large animal. *European Cells & Materials*, *41*, 546–557.

<https://doi.org/10.22203/eCM.v041a35>